Solar Electric Propulsion System Evaluation

E. V. Pawlik,* E. N. Costogue,† J. D. Ferrera,‡ and T. W. Macie§
Jet Propulsion Laboratory, Pasadena, Calif.

The design and experimental evaluation of a solar-electric primary propulsion system is described. The system consists of two electron-bombardment ion thrusters complete with the associated thrust-vector aligning actuators, a switching network, controller, and a flight-type power conditioner. The system was operated over a 2:1 range in output power. System integration problems such as matching of thruster performance and response to arcing within the thruster and solutions to these problems are described. A 252-hr shakedown test and a 298-hr endurance test of the system were conducted. Noise within the system was the major lifetime-limiting factor for both the power conditioner and controller.

Introduction

THIS report describes the design and testing of an electric propulsion system that incorporates the minimal features considered necessary for the primary propulsion system of a solar-powered, electrically propelled, deep space probe. Most major elements necessary for a solar-electric system were present. The system was essentially a breadboard arrangement that could form a baseline design for early electric propulsion flight systems. The objective of these tests was to identify problems associated with system integration and to develop solutions.

The capabilities of the system included: 1) closed-loop stable operation of a thruster, neutralizer, and power conditioner, 2) control of thrust power over a 2:1 range by means of a single command signal, 3) remote starting and stopping of the power conditioner/thruster system, 4) remote reconnection of the power conditioner to a spare thruster, 5) automatic recycle of the system to clear sustained arcs within the thruster, 6) single-axis thruster gimballing, 7) single-axis translation of the thrust vector, 8) detection of failures in the power conditioner/thruster set, and 9) generation of the required telemetry signals.

The system has been integrated and has undergone shakedown and some endurance testing, accruing 550 operating hours. The details of the system, component integration, and system testing are described.

System Design

The propulsion system employed two 20-cm-diam electron-bombardment ion thrusters utilizing mercury propellant and was designed to operate over a 2-to-1 range in output power to permit impedance marching to a solar array with a varying solar constant. All operation was at a fixed nominal specific impulse of 4000 sec. Each thruster was gimballed to provide ±10 deg of thrust vectoring about one axis. Therefore, when operated in pairs during flight, the thrusters could provide the necessary couple about the roll axis for attitude control. Thrusters, neutralizers, and gimbals were mounted on a common structure which could be translated along one axis to permit adjustment of the thrust vector position. The thruster, neutralizer, and actuator portions of the system were mounted in a vacuum chamber (Fig. 1). A schematic representation of the entire system is shown in Fig. 2.

A single, lightweight, modular power conditioning unit was employed to convert the simulated solar array power to the various inputs necessary to operate the thruster. This unit, developed under contract by the Hughes Aircraft Company, was capable of operating either in atmosphere or in thermal vacuum. A switching network allowed either thruster to be connected to the power conditioner or to laboratory power supplies. Failure of either the power conditioning unit or ion thruster was detected by a controller.

The system elements will each be described in detail. The weights of elements used are presented in Table 1. It is believed that these weights can, in most cases, be reduced considerably.

Ion Thruster, Neutralizer, and Mercury Feed

The thruster (Fig. 3) was designed to operate at a nominal input power of up to 2.5 kw and is, with small modifications, the same thruster as described in Ref. 1. A nominal net accelerating voltage of 2 kv was employed, and with operation normally at 90% propellant utilization, this corresponds to a specific impulse of 4090 sec. The normal operating region for ion beam current was 0.5 to 1.0 amp. An oxide cathode

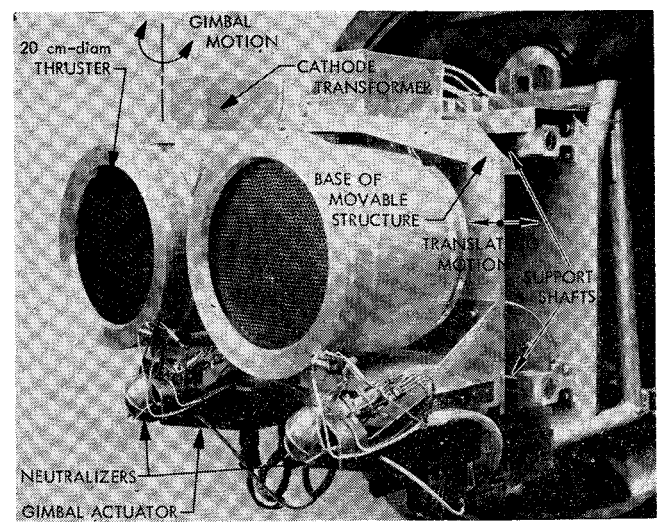

Fig. 1 In-tank portion of the propulsion system.

Presented as Paper 69-498 at the AIAA 5th Propulsion Joint Specialist Conference, U.S. Air Force Academy, Colo., June 9–13, 1969; submitted July 7, 1969; revision received April 6, 1970. This paper presents the results of one phase of research carried out in the Propulsion Research and Advanced Concepts Section of the Jet Propulsion Laboratory, California Institute of Technology, under Contract NAS 7-100, sponsored by NASA.

* Senior Engineer, Propulsion Research and Advanced Concepts Section. Member AIAA.
† Member Technical Staff, Spacecraft Power Section.
‡ Engineer, Spacecraft Control Section. Member AIAA.
§ Member Technical Staff, Propulsion Research and Advanced Concepts Section.

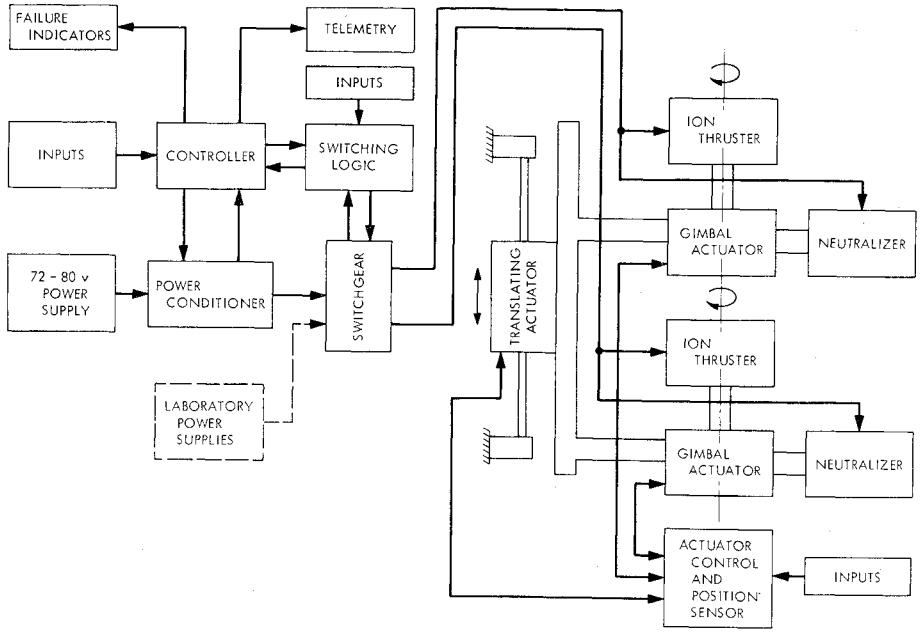

Fig. 2 Schematic diagram of the solar-electric propulsion system.

was used for the electron source within the thruster because of its availability and knowledge of its characteristics. A hollow cathode[2] or liquid mercury cathode[3] now appears to be a more attractive selection for the primary electron source from the standpoint of both cathode power and lifetime, and will be utilized in future tests.

The changes in the thruster design that were incorporated during this study were use of 1) tapered accelerator grids and 2) 3 screen grid braces. Accelerator grid thickness decreased with the radial distance from its center, so that more material could be placed in the region where the greatest wear is normally observed. The three grid braces were used to reduce the grid separation variations due to thermal loading and the attendant effects on ion chamber performance. This design exhibited essentially no movement during bench thermal tests.

The cesium-plasma bridge neutralizer developed by Electro-Optical Systems[4] was the only available plasma bridge neutralizer which operated on an acceptably low propellant flow rate. Neutralizer selections for flight will be based both on performance and on materials interactions. A cone-half angle of 40° was assumed for the total spread of the ion beam, based on data for a similar thruster in Ref. 5. The neutralizer was directed 45° downstream and was placed so as to be slightly removed from the beam edge when the thruster was gimballed toward the neutralizer.

Mercury flow to the thrusters was driven by one atmosphere pressure from an external burette that permitted calibration of the vaporizers during thruster operation. The burettes would not be used in a flight system. Propellant flow from the reservoir passes through a latching solenoid valve which requires power only during opening or closing. This valve is a desirable feed system feature to contain the mercury during launch and to stop flow to standby thrusters. The vaporizers were connected to the burette by 0.16-cm-o.d., 0.015-cm-wall stainless steel tubing. Each propellant feed line contained 2 23-cm-long loops to provide the necessary flexibility across the movable interface.

Table 1 System weight breakdown

Component	Weight, kg
Cathode transformers (two)	0.84
Gimbal actuator	1.95
Latching valves (two)	0.50
Neutralizers (two)	0.71
Power conditioning unit	14.97
Power conditioner cable and connectors	2.27
20-cm-diam ion thrusters (two)	7.90
Thruster wiring and connectors (to connector bulkheads, two sets)	2.00
Structure (movable portion)	8.75
Switchgear (total of four)	2.95
Translating actuator	3.29
Controller (including failure logic)	1.80
Total weight, kg	47.9

Power Conditioner

A previously developed power conditioner[6] was modified for use with the thruster. Modifications included 1) an increase in the total power level, 2) different control loops, 3) regulation of arc and magnet supplies, 4) incorporation of neutralizer power supplies, and 5) a redistribution of the power levels. The resulting power conditioner delivered a nominal power of 2450 w and had a maximum power handling capacity of 2800 w. The input voltage could range from 72 to 80 vdc. The 25.3- × 37- × 6-in. unit weighed 38 lb (including ~5 lb for cables and connectors) and consisted of 30 individual modules, including redundant units, mounted on a supporting frame.

The modular system has a low specific weight because the individual modules operate at low power levels, for which high-frequency transistors are available. Most of the inverters operate at 12 kHz, which reduces the size and weight of all the magnetic components. High efficiency is possible because the individual components are operated at low specific stress, so the losses in all the semiconductors and magentics are very low. Because of the low-power dissipation of each module, the mounting chassis can dissipate all the losses by direct radiation to space without additional heatsinks or radiators. The multimodule system also offers great flexibility; in the case of a failure, changeover from a working module to spare module is performed electronically by means of a command generated by internal failure logic. The main building blocks (Fig. 4) and features are as follows.

1) Accelerator power supply, comprising two modules, one operating and one on standby. The modules contain a free-running inverter followed by a transformer rectifier circuit. The converter also provides square-wave drive for the arc and screen inverters.

2) Screen power supply, comprising seven converters connected in series. An eighth converter is on standby. A common filter is used for all the units.

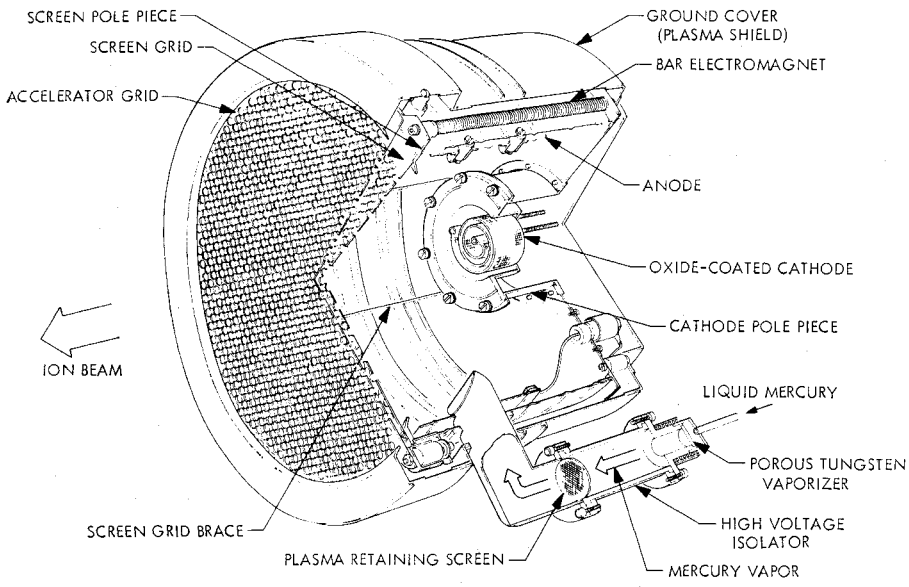

Fig. 3 20-cm (anode) diameter thruster.

3) Arc power supply, comprising two modules, one on standby. It is a closed-loop, voltage regulated supply.

4) Modulator subsystem, comprising a free-running inverter at 5 kHz that supplies the power to four modulator circuits. The modulators were the power supplies of a) neutralizer keeper, b) magnetic manifold heater, c) thruster vaporizer, and d) neutralizer vaporizer and cathode heater. A common preregulator compensates for line voltage variations. The subsystem inverter also supplies drive for the cathode supply.

5) Cathode heater power supply, comprising two modules, one on standby. Each module contains a driven inverter with a magnetic amplifier for duty cycle control. The output transformer is remotely located to reduce transmission losses and to improve regulation.

6) Self-protection; most low-voltage power supplies are short-circuit-proof to prevent damage by an overload. Excessive current to the arc or high-voltage supplies would cause it to shut down and restart a short time later (initially on the order of 1 sec).

7) External control to a) start the system, b) regulate the level of power delivered to the thruster, and c) shut down the system.

8) Three servo loops to control thruster output power and propellant flows, namely, the neutralizer, beam current, and cathode-arc current loops. The thruster control loops have been analyzed and are discussed in Ref. 7. The need to control the propellant utilization accurately imposes tight (1% or better) output regulation requirements on the power conditioner; operation at high propellant utilization (90% or better) eases this requirement slightly.

9) Telemetry for all parameters that are considered essential for determining the proper functioning of the ion thruster.

Switching Matrix

The power conditioning unit could be linked to either of the two ion thrusters by means of multiple-contact, multiple-deck selector switches. Because of weight considerations, the design permitted switching only when the power conditioner was turned off. Two switches were required per power conditioning unit. The four switches used in the system also permitted the laboratory power supplies to be connected to either thruster.

The switchgear was operated by a remote control unit equipped with switching logic to permit the specification of thruster and power conditioner combination. The electronic circuitry provided the required interlocks inhibiting switching when the power conditioner was energized and provided a signal to the controller that prevented operation of the power conditioner if the switching operation malfunctioned.

Controller

This unit served 1) to provide command signals to the power conditioning unit, 2) to monitor telemetry outputs, 3) to detect failure of either the ion thruster or power conditioning unit, and 4) to inform switchgear logic when power conditioner was on. In providing the command signals, it sequences the starting of the system, generating a preconditioning sequence for the cathode and neutralizer. It also specifies the level of the ion beam power. A logical extension of this unit would be, upon detecting failures, to direct the operation of the switchgear.

The failure detection unit monitored only the ion beam current and the screen and accelerator voltages. A failure was defined as a deviation of any of these parameters greater than $\pm 10\%$ of their specified values 3 sec or more.

The ion beam current level during system operation was variable, since 1) the steady-state value could be specified within a 2:1 range and 2) the initial thruster turn on retards the ion beam from reaching the lower limits of its operating range because of the long thermal time constant of the ion thruster. For this latter reason, the controller must time sequence the turn on of the beam failure detection. The lower limit of the failure monitor is initially zero after thruster turn on and is increased incrementally in each of the next 3 30-min periods.

The assigned functions of the failure logic system are performed by means of commercially available micrologic cards. These logic cards are included in Table 1 as the controller weight.

Thrust Vector Control

The thrust vector control consisted of the actuators and control electronics. This part of the system was constructed to demonstrate proof of concept regarding precision, reliability, and system compatibility. Flight environment and weight requirements were given secondary attention. The mounting of the gimbal and translating actuators on the in-tank portion of the propulsion system is shown in Fig. 1.

The unique feature of the gimbal actuator was the drive arrangement utilized to minimize backlash between the output shaft and feedback pickoff in order to obtain a design goal of 0.1 mrad (20.6 arcsec) of shaft rotation per stepper motor step input. The linear motion of the saddle nut due to the lead screw was transformed to rotary motion of the

output sector through two beryllium copper straps. The saddle nut was also pinched slightly prior to machining of screw threads such that, in its assembled state, the saddle nut screw threads were forced into contact with the lead screw threads. A solid rod connected the saddle nut to the pickoff arm. Thus, there was essentially zero backlash between the actuator output shaft and the position pickoff. The position pickoff was a linear variable differential transformer which sensed lead screw position. To reduce heat conduction from the thruster to the actuator, an intermediate shaft connecting the two was made of stainless steel rather than aluminum. With the exception of the straps, all other parts of the actuator were made of aluminum. The lead screw itself was a hollow aluminum shaft, hard-anodized after machining. For the system testing of the actuator, six thermistors were attached internally to monitor temperature during thruster operation. The actuator case was a sealed unit and was pressurized to 5 psia using a 90% N_2, 10% H mixture. Static seals were provided by a single 0-ring. The dynamic output shaft seal was accomplished by using two 0-rings separated by a lubrication groove.

Two features of the translation actuator are particularly noteworthy. One is the application of a harmonic drive gear train to obtain very low values of backlash (less than 5 arcsec) and high output torsional stiffness; this low backlash is obtained through careful selection and matching of component parts. The other is the platform drive external to the actuator. This motion was accomplished by the use of

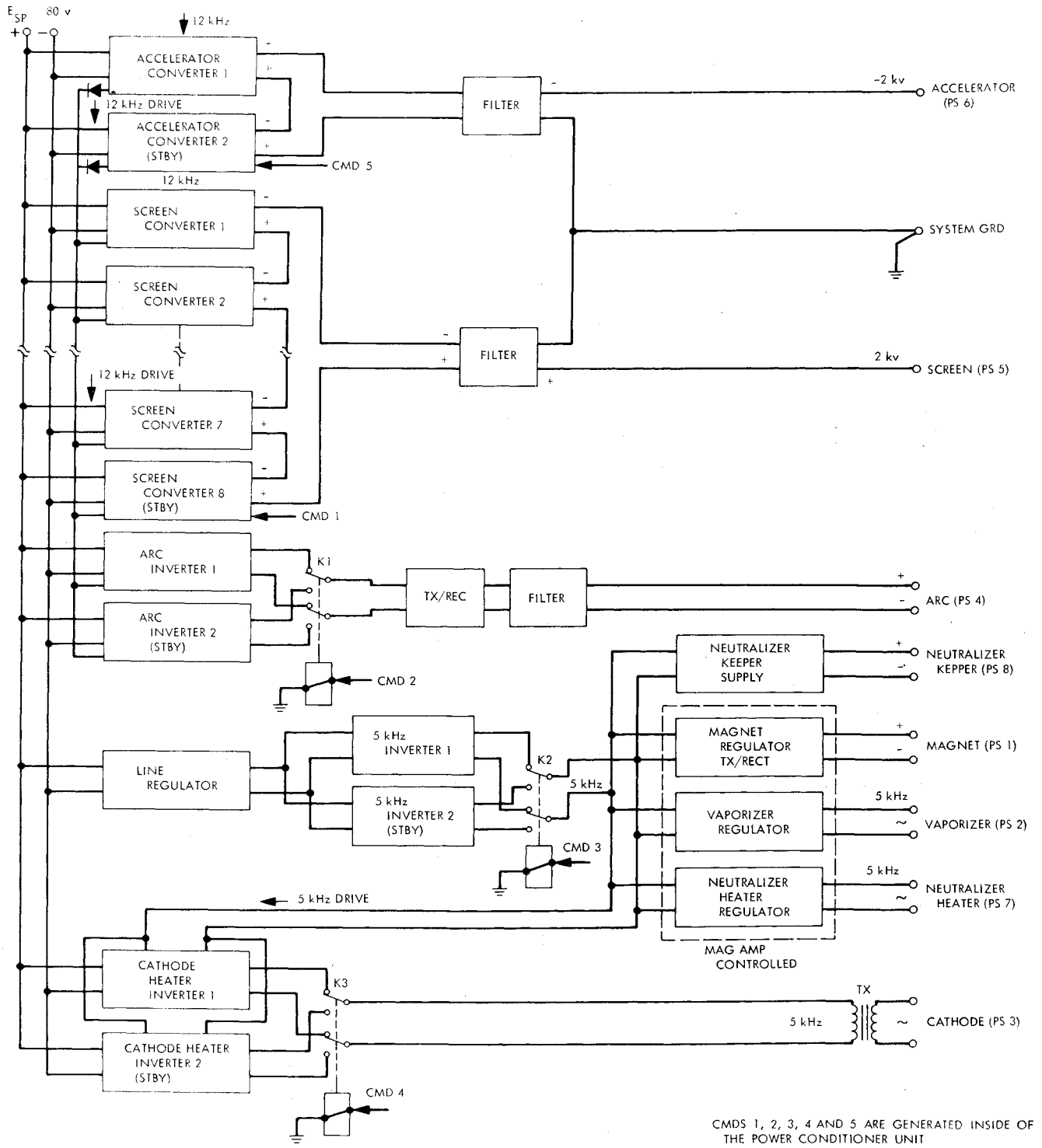

Fig. 4 Power conditioner block diagram.

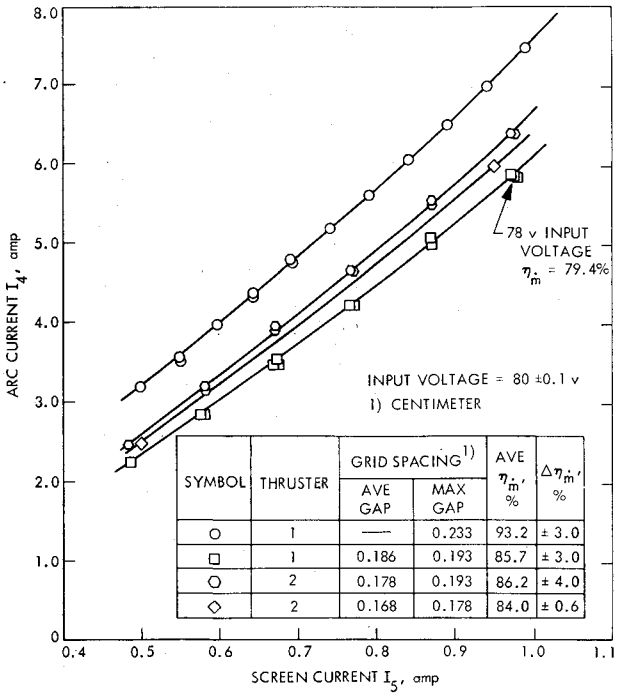

Fig. 5 Curve-matching of two thrusters.

a flat-strap type of drive that connects the output drum to stainless steel roller bearings which ride on parallel, stainless steel shafts. Fatigue cracks that might develop in the strap drive are self-healing in a space vacuum. It is anticipated that ceramic balls will be used in the roller bearings to eliminate the possibility of cold welding of similar metals in a space vacuum. Mechanical stops on the stainless steel rods limited mechanical travel to ±7.5 cm for the system tested. The system was capable of 33 cm of travel when removed from the vacuum chamber. The gear ratio provided 0.0064 cm of output translation per stepper motor step. A rotary infinite resolution potentiometer was used for position feedback.

A thrust vector control unit provided open loop actuator control and test instrumentation. Operation of only one gimbal or the translating actuator at a time was permitted. Actuator stepper motor speed rates of 5, 50, or 100 steps/sec in addition to single-step operation were available. A selector switch permitted either test or run mode of operation. The run mode was used primarily for endurance testing, automatically reversing the actuator direction when the electrical stop was reached.

Mounting Structure

An aluminum structure was used to mount the ion thrusters, gimbal actuators, translator actuator, cathode transformers, and neutralizers. The construction consisted mainly of thick, flat members, providing a rigid structure. All removable support arms were pinned to provide accurate alignment during assembly.

System Integration

The system was operated to evaluate the design of various elements and to study integration problems. The in-tank portion of the test was performed in a 3 × 7-ft vacuum chamber maintained at a pressure of 6×10^{-6} torr. Since the system operation was maintained for lengthy intervals, sputtered material from the tank walls coating the experimental setup was a problem. A movable cover was employed to protect the nonoperating ion thruster from some of this contamination.

Ion Thruster

Two thruster problem areas were encountered during integration with the power conditioner. These concerned thruster performance reproducibility and transient currents during turn-on. Furthermore, high steady-state operating levels of output power were unobtainable due to large transient currents within the arc, beam, and accelerator power supplies during re-establishing of thruster operation after a sustained arc between the accelerator grids.

Thruster performance variations

Because of the unavailability of a reliable and accurate mercury flowmeter, the utilization of the mercury propellant was derived indirectly from the measurement of the electrical power dissipated in the ion chamber. The control of the propellant flow depended upon the ability to maintain the mass utilization at a constant value for all levels of beam current. Utilization of a single command for beam reference set point was possible by employing a functional relationship to specify the arc current for each beam current level. The power conditioner was therefore provided with a function generator that converts the beam reference signal into an arc reference signal and reproduce a single constant propellant utilization efficiency curve (nominally 90%). Functional requirements of individual thrusters varied because of construction differences. Each thruster required its individual functional curve or else a correction for thruster differences was necessary.

During ion thruster testing it was observed that highly repeatable data from either the same or a similar thruster were difficult to obtain. A 5% or greater variation in discharge losses have commonly been observed during performance mapping. The similar thrusters were identical except for mechanical tolerances held during manufacture and small variations that existed in assembly. Sources of performance discrepancies that have been identified to date include 1) small variations in electrical parameters, 2) hysteresis in the magnetic material, 3) uncertainty associated with the flow measuring technique, and 4) variations in the screen-accelerator grid geometry.

The variations in electrical parameters and hysteresis in the thruster permeable paths were both minimized by operating from the power conditioning unit while maintaining the input voltage at a fixed value. Repeatable, if not highly accurate, flow measurements were also obtained during the operation of either of the two thrusters. Variations

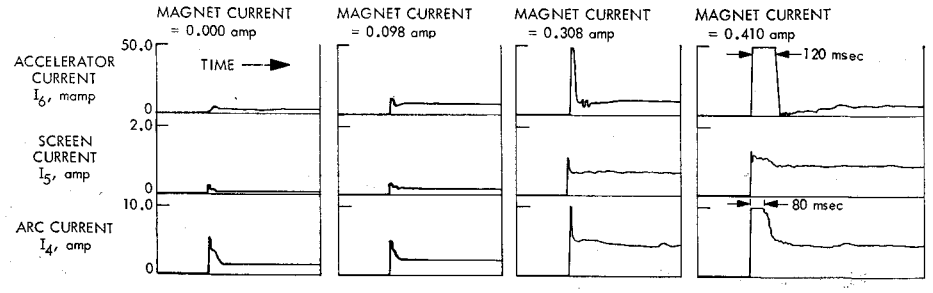

Fig. 6 Accelerator, screen, and arc currents during discharge initiation with laboratory power supplies.

in ion chamber performance still existed between the two thrusters, however.

The ion chamber performance can be affected by the ion extraction system and therefore constant grid geometry is critical to repeatable thruster performance. Variations in the grid geometry such as thickness, spacing, and hole diameter are sources of errors.

The data presented in Fig. 5 show the functional relation between the arc current and the beam current over a 2:1 range of output for two nonidentical ion thrusters. The thrusters were operated from the power-conditioning unit with the input voltage set at 80.1 ± 0.1 v, which resulted in close-setting of all electrical inputs.

Differences in performance were observed as the uniformity of the gap between the accelerating grid structure was altered. Similar thruster performance was approached by adjusting the screen grid braces. Small remaining variations could be minimized by further changes in the average grid separation, allowing either of the thrusters in the system to operate from the power conditioner without adjusting the function generator.

The input-line voltage was dropped by 2.5% (2 v) to demonstrate the need for close control of the thruster parameters. For this power conditioner this was the simplest way of varying the nonregulated outputs. This change caused a 2.5% reduction of all nonregulated outputs. Operating the thruster along the same functional curve as for the nominal line, at the point indicated in Fig. 5, resulted in lowering the propellant utilization to 79.4% from 83.8%. As the input-line voltage was decreased further (by 4 v or more), changing the unregulated outputs by 5% or more, the propellant flow could no longer be controlled and continuously increased, resulting in a runaway condition.

Recovery from arcing

In order to clear a sustained arc, the circuits in which the arc appears were interrupted to allow time to extinguish the arc. Igniting of the plasma within the thruster was observed to present high intensity surge currents in the arc, screen, and accelerator circuits. These surges were usually higher than the protective circuitry of the power conditioner would permit. A way of minimizing these currents to present a "soft start" for the power conditioner was therefore sought.

The overcurrent surges were examined in detail and subsequently focused attention on the pressure within the ion chamber as the main cause of these high current conditions. The intensity of these surges has been demonstrated by changing thruster flow rates to be proportional to the ion chamber pressure. Reduction of the ion chamber pressure or a decrease in the density of the plasma at high-pressure conditions are the approaches that are presently proposed for minimizing these surges. Some of the tests that have been run with laboratory supplies to arrive at these conclusions are described below. These test data were obtained by interrupting thruster operation and then initiating the discharge shortly thereafter.

The ion chamber plasma density is a function of the magnetic field. Figure 6 shows how the intensity of the magnetic field (or plasma density) affects the amplitude and duration of overshoots of the three currents that have trip limits within their circuits. It became evident that the most desirable way to restart thruster operation is to do so without any magnetic field.

Ion chamber plasma density could be further reduced by decreasing either the arc voltage or current. The range of arc voltage adjustment is limited, and therefore only a current reduction was examined. The arc current can be reduced by lowering the cathode heating power. Tests were run in order to determine how temperature of the cathode affects the magnitude of current overshoots. Marginal benefit was found to be derived from reducing the cathode power.

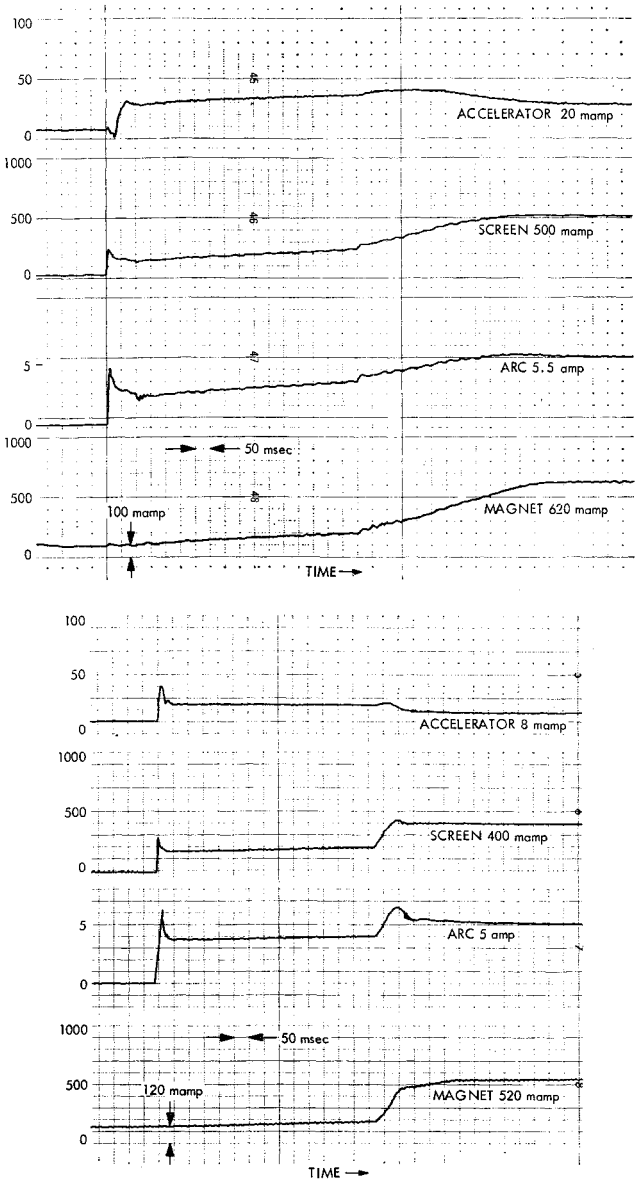

Fig. 7 Power conditioner discharge initiation as a function of magnet ramp.

The mercury flow rate was also investigated and found to greatly affect the overshoots. It is most desirable to restart with a reduced rate of flow. Finally, it was also found that the rate at which the magnet current is raised can lead to undesirable overshoots. Figure 7 presents the currents observed as different rates of magnet current increase were employed. Ramp times of 0.6 sec or longer provided essentially no overcurrent conditions.

Neutralizer and Mercury Feed

The operation of the neutralizer with the thruster was mapped during operation with the power conditioning unit. The keeper voltage was maintained at 5.2 v. The cesium flows for this set point were derived from an extrapolation based on the flow rate as measured at EOS during an endurance testing with this type of neutralizer; flow rates were on the order of 0.09 g/hr. The bias voltage necessary to maintain the neutralizer emission equal to the beam current as the thruster was gimbaled is presented in Fig. 8 for two values of beam current. Low voltage levels of neutralizer-to-beam coupling were found to exist for all values of gimbal position. These voltages were considerably below the 30-v level where detrimental wear has been observed.[5] The

DATA POINT SYMBOL	BEAM CURRENT, amp	NEUTRALIZER VAPORIZER TEMPERATURE, °C	NEUTRALIZER CESIUM FLOW, g/h	THRUSTER MERCURY FLOW, g/h
○	0.480	328	0.087	4.00
□	0.913	331	0.091	7.61

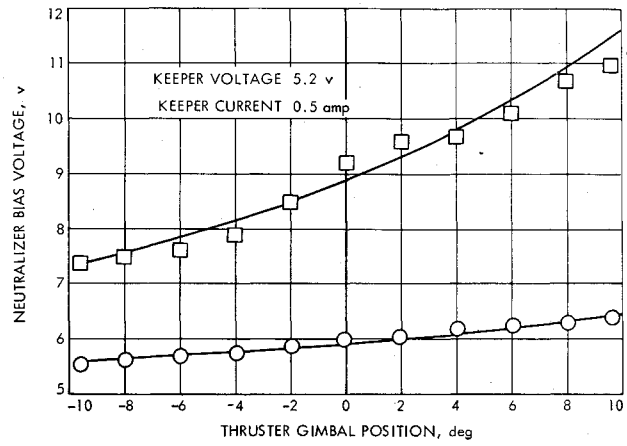

Fig. 8 Neutralizer coupling voltage as a function of thruster gimbal angle.

cesium flow was calculated to be 1.2 to 2.2% of the ion beam.

No problems were encountered with the flexible Hg feed lines. The latching valves exhibited a very slight (0.27 g Hg/24 hr at 45 in. Hg head) leakage through the valve when in the closed position after an estimated 5000 operating cycles.

Power Conditioner

The power conditioner was evaluated on a test console before integration testing. The evaluation test included the measurement of the power supplies, regulation characteristics, the verification of logic controls, and the evaluation of the operational characteristics of the control loops.

The test console was equipped with a number of special features. These included 1) variable dummy load to verify the characteristics of each supply, 2) high voltage breakdown vacuum relays to check the performance of each power supply under transient conditions, and 3) digital and analog signal generation to initiate command and set the operational levels of the power conditioner control loops. Data taken during this test indicated that the power-conditioning unit was 90% efficient.

The power conditioner supplies were initially evaluated with the ion thruster with the control loops opened and then these loops were closed sequentially. Difficulty in restarting, and problems encountered later during endurance testing led to modifications as follows.

1) The magnet supply was equipped with a delay and ramp circuit to drop the magnet current to a minimum value of approximately 75 mamp with a time constant of 50 msec, to maintain the minimum value during the delay time of 1 sec, and to ramp to the full magnet current in 0.5 sec. The delay and ramp circuit was activated by the logic sensor detecting a sustained arc. The delay circuit was finally adjusted to provide three seconds of delay plus ramp time. To assure that magnet delay and ramp circuit will be energized by the tripping logic, an OR gate was introduced. A signal input from the accelerator supply was introduced in addition to the trip signal.

2) The overcurrent trip sensors were redesigned to eliminate unnecessary tripping responding to an intermittent, nonsustained arcing that did not require system shutdown. The adjusted levels of overcurrent trip sensors and tripping delays were: arc current = 7.5 amp, 10 msec; beam current = 1.09 amp, 2 msec; accelerator current = 106 mamp, 5 msec.

3) The gain and phase margin of the cathode-arc operational amplifier were adjusted to eliminate oscillation noticed during closed loop operation. An open-loop gain much greater than 100 resulted in a small undamped oscillation in this loop. This result was not predicted in the analytical model of the system.

4) A negative feedback loop was introduced in the cathode-arc operational amplifier to compensate for the true arc current sensing. The current transformer in the arc supply measured the summation of arc end beam current. To subtract the beam current, a proportional input from the beam sensing circuit was obtained and introduced in the cathode-arc operational amplifier.

5) After the shakedown testing, the vaporizer and the cathode supplies were equipped with circuits to delay their currents after overcurrent trips by 2 sec and 1 sec, respectively, and a circuit was introduced to stop the internal power conditioner clock for a period of 100 to 450 msec after an overcurrent trip, so that the high voltage supplies would not start until after a minimum delay of 100 msec, allowing time for the magnet current to decay.

Closed-Loop Servo Control

From earlier theoretical studies,[7] it was found that very close control of all electrical parameters is needed in order to retain close control of the consumption of mercury. Mass utilization was specified to be near 90%, and variations in voltages were minimized by maintaining the input voltage at a fixed value. The original loop gains for both I_3/I_4 and I_2/I_5 were measured to be near 250, but I_3/I_4 was unstable with this gain, resulting in continuous oscillations in the beam current. Reduction of the gain to 100 was necessary to eliminate this condition.

Typical closed-loop system operation is shown in Fig. 9. The reference set point was abruptly changed several times to indicate the response of the system; after 42 min of operation the system was completely turned off with an OFF-2 command. The system was turned on 11 min later and automatically restored normal operation. An OFF-1 command was given after 66 min which turned off only the vaporizer, allowing the thruster operation to decay.

Electrical interference

The operation of an ion thruster generates a considerable amount of interference. Even during stable operation of the thruster, with all of the regulating loops responding quickly

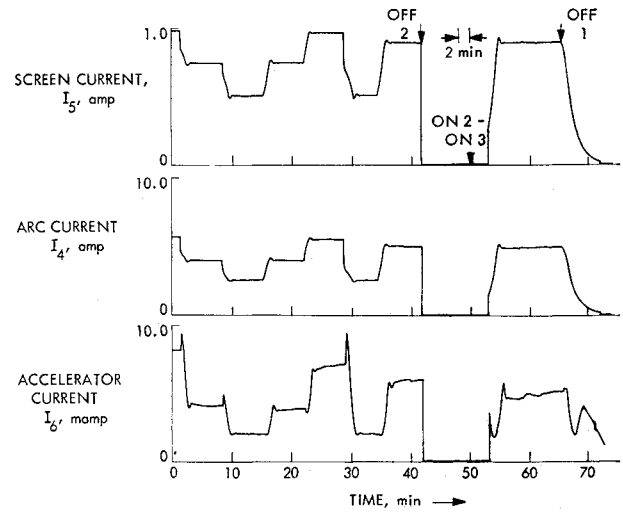

Fig. 9 Closed-loop system operation.

and accurately, there is evidence of periodic arcing between various portions of the thruster. Either sustained or self-extinguishing arcs form a source of interference, the effects of which have to be minimized.

Currents changing at a high rate generate high-frequency electromagnetic fields that may induce currents in other conductors of the same harness or be picked up by various loops of wiring that act as receiving antennae. Since the magnitude of the signal generated within the receiving antenna is proportional to the area enclosed by the loop, an effort to minimize such loops was made.

All the signal grounds were attached to a single-signal ground ring which is connected to the common tie point of all the power grounds within the power conditioner. A single line connected the signal ground ring with each of the individual modules; all of the ground connections of the particular module were made to that common line.

In spite of the above precautions, considerable noise was recorded on all dc lines inside the power conditioner logic (Table 2). In some cases the noise levels were above the published component steady state limits and could cause the failure of components that are exposed to them. Further clarification of transient limits and improved protection is required.

The magnitude of radiated noise may be considerably diminished by close-coupling the feed and return lines magnetically. It is felt that this was partially accomplished by inclusion of the return lines in the power harness. It is recognized that further improvements are required and could be attained by using twisted pairs and proper shielding.

System performance also may be affected by the conducted interference. As described earlier, most of these nuisance trippings were eliminated by desensitizing the sensing circuits and slowing down their response; no tripping of the power conditioner occurred in cases where arcing was not of a sustained nature and lasted less than 5 msec. To eliminate errors in telemetered data filtering was added at the input of the controller.

Transformer

The cathode transformer supplied with the power conditioner was mounted on one thruster and a larger transformer constructed at JPL was mounted on the second. Sputtered material proved somewhat troublesome for both designs and extensive shadow shielding was required. The major problem for both transformers was the heat conducted along the leads connecting the secondary windings to the cathode. Temperatures at the transformer as high as 265°C were recorded. Redesign of the transformer to withstand higher temperatures was necessary.

Switching Matrix

Noise generated by the power conditioner and ion thruster caused the logic and position indicators to malfunction.

Table 2 Noise levels present in power conditioner electronics

Nominal DC level, *v*	Location	Permissible maximum component stresses, *v*		Transient stresses observed, *v*
		Steady state	1-sec	
4.5	Control	8	12	4.7
6	Control			8.1
	Arc	8	12	8.9
	Accelerator			10.5
12	Control	18	[a]	17.5
40	Control	100	...	57

[a] Data not available.

Table 3 Noise level present on controller critical lines[a]

Checkpoints	Steady-state level, *v*	Transient level, *v*
d.c. input	+15	25
d.c. input	−15	−23
Negative reference	5.5	16
E_6 TM	7.4 max	17
TM ground	Near zero	16

[a] All measured to chassis ground.

No switching of interconnections was triggered by this noise environment. Commanded switching arrangements were successfully completed since the switching took place when the power conditioner and thruster were inoperative. Filter networks were introduced in the input lines of the unit to reduce the level of the noise present. With these filters in the system, the position sensors were unaffected by the system noise levels.

Controller

Two changes were found to be necessary when integrating the controller into the system.

1) Filters were added to the input lines, because the noise immunity of the controller was not adequate, and the failure indicating lights turned on erratically. Table 3 lists the recorded levels of noise present before filtering was added. By modifying the signal ground connections and filtering the incoming lines, the noise pickup was brought within the allowable steady state limits and false indications were eliminated.

2) The time during which a measured parameter was allowed to remain outside of the acceptable range was increased from 3 to 4 sec to eliminate false failure indications.

Thrust Vector Control

Two minor problems developed relative to the actuators. 1) A slight buckling of the gimbal actuator housing resulted in the binding of this actuator, which therefore failed to rotate the thruster; this problem was eliminated by adding supports to the two ends of the lead screw bracket. 2) A high leak rate was found in the gimbal cover seal where the ends of a split 0-ring were butted together with epoxy; this problem was eliminated by replacing the 0-ring with one constructed with a vulcanized joint.

Table 4 Maximum component lifetimes obtained during system testing at JPL

Component	Exhibited lifetime during system testing, hr	Major lifetime limitation
Ion thruster	220	Facility sputtering (metal coating)
Neutralizer	114	Improper handling procedures
Controller	220	System noise
Power conditioner	195	System noise
Gimbal actuator	121 (12.2×10^6 steps)	None encountered
Translating actuator	32 (8.30×10^6 steps)	None encountered
Actuator electronics	200	None encountered
Switchgear	1000 (500 estimated operations)	None encountered
Switchgear electronics	600	None encountered
Latching valve	... (5000 estimated cycles)	None encountered

Table 5 Endurance test—total steps accumulated/actuator

Component	Mission requirements, steps	Accumulated in test, steps
Translation actuator	$<6.35 \times 10^6$	8.30×10^6
Gimbal actuator 1	$<6.35 \times 10^5$	121.25×10^6
Gimbal actuator 2	$<6.35 \times 10^5$	24.0×10^6

A system interaction was observed during movement of both actuators as the beam and accelerator currents varied with position. The vaporizer flow rate was apparently sensitive to the system motion suggesting a partial mercury penetration into the vaporizer or a vapor pocket in the feedline.

System Testing

After the problems described in the previous section were corrected, a shakedown run of 252 hr was made, during which system faults were discovered and corrected. Then an endurance test of 298 hr was performed.

Very few problems were found in the power portion of the power conditioner; most were found within the logic. The maximum demonstrated lifetime of the power conditioner and each of the other system components is listed in Table 4. The actuators were the most successful component tested, meeting lifetime requirements as shown in Table 5. Severe facility limitations, in the form of backsputtered material from the vacuum tank walls generated in stopping the high-velocity ion beam, prevented long thruster lifetimes and also presented a strenuous power conditioner evaluation by causing excessive thruster arcing. Sputtered material coated all electrical connections and insulators, requiring excessive shadow shielding. The thruster cathode could not be shielded, and this eventually resulted in the failure of thruster 1.

The light weight of the power conditioner unit and the excessive number of modifications during the described and previous program reduced the quality of the unit substantially. However, system noise was the major lifetime limiting factor for both the power conditioner and controller.

Conclusions from this program of system integration and testing are as follows.

1) The discharge chamber power of an ion thruster, necessary to provide a specified output power and propellant utilization, may be adjusted to some extent by modifying the gap spacing between accelerating grids. This adjustment allows slightly different thrusters to be trimmed so as to give identical operation from a given power conditioning unit.

2) The use of an ion thruster employing electromagnets provides system advantages. Control of the thruster magnetic field provided convenient control of the plasma density within the discharge chamber, permitting a "soft" restart of the system. This restart procedure minimized transient overcurrents observed to be present during both initiation of a discharge and during restoration of the strength of the magnetic field.

3) Closed-loop control of a system was demonstrated to be possible for a continuous 2:1 range of output power, while maintaining propellant utilization in the neighborhood of 90%.

4) Electrical interference generated the ion thruster, and power conditioner was found to be a source of integration problems. This interference was reduced to a tolerable level by introducing line filters, shielding, and by minimizing the area of all loops that could serve as receiving antennas. The levels of noise inside the electronic circuits were not compatible with high reliability requirements and long term degradation may be expected. This limitation could be eliminated by designing proper noise protection into the logic system.

5) Short-term endurance of "shakedown" system testing with a thruster exhibiting a high rate of arcing is an effective method for detecting system weaknesses. In this type of environment, power conditioner weaknesses are rapidly discovered, providing a form of accelerated system life testing.

6) Although some of the foregoing require further investigation, no fundamental limitations were uncovered. It is believed that with a reduction in backsputtered material (by the use of a larger vacuum facility, for example) and with system electronics constructed of high-reliability components and with noise immunity designed in, system lifetimes compatible with flight requirements will be achieved.

References

[1] Masek, T. D., "Evaluation of the SE-20C Thruster Design," *Space Programs Summary 37-51*, Vol. III, June 30, 1968, Jet Propulsion Lab., Pasadena, Calif.

[2] Masek, T. D. and Pawlik, E. V., "Hollow Cathode Operation in the SE-20C Thruster," *Space Programs Summary 37-5*, Vol. III, Oct. 1968, Jet Propulsion Lab., Pasadena, Calif.

[3] Hyman, J., Jr. et al., "Liquid-Mercury Cathode Electron-Bombardment Thrusters," AIAA Paper 69-302, Williamsburg, Va., 1969.

[4] Sohl, G., Fosnight, V. V., and Goldner, S. J., "Electron Bombardment Cesium Ion Engine System," Summary Report on NASA Contract CR-54711, Rept. 6954, April 1967, Electro-Optical Systems, Pasadena, Calif.

[5] Rawlin, V. R. and Pawlik, E. V., "A Mercury Plasma-Bridge Neutralizer," AIAA Paper 67-670, Colorado Springs, Colo., 1967.

[6] *Development and Test of an Ion Engine System Employing Modular Power Conditioning*, Project Final Report SSD-60374-R, Sept. 1966, Hughes Aircraft Co., Culver City, Calif.

[7] Mueller, P. A. and Pawlik, E. V., "Control Analysis of an Ion Thruster with Programmed Thrust," AIAA Paper 69-239, Williamsburg, Va., 1969.